

# We are IntechOpen, the world's leading publisher of Open Access books Built by scientists, for scientists

6,900

Open access books available

185,000

International authors and editors

200M

Downloads

Our authors are among the

154

Countries delivered to

TOP 1%

most cited scientists

12.2%

Contributors from top 500 universities



WEB OF SCIENCE™

Selection of our books indexed in the Book Citation Index  
in Web of Science™ Core Collection (BKCI)

Interested in publishing with us?  
Contact [book.department@intechopen.com](mailto:book.department@intechopen.com)

Numbers displayed above are based on latest data collected.  
For more information visit [www.intechopen.com](http://www.intechopen.com)



# Prediction of Elastic Properties of Plain Weave Fabric Using Geometrical Modeling

Jeng-Jong Lin

*Department of Information management, Vanung University  
Taiwan, R.O.C.*

## 1. Introduction

Fabrics are typical porous material and can be treated as mixtures of fibers and air. There is no clearly defined boundary and is different from a classical continuum for fabrics. It is complex to proceed with the theoretical analysis of fabric behavior. There are two main reasons (Hearle et al., 1969) for developing the geometrical structures of fabrics. One is to be able to calculate the resistance of the cloth to mechanical deformation such as initial extension, bending, or shear in terms of the resistance to deformation of individual fibers. The other is that the geometrical relationships can provide direct information on the relative resistance of cloths to the passage of air or light and similarly it can provide a guide to the maximum density of packing that can be achieved in a cloth. The most elaborate and detailed account of earlier work is contained in a classical paper by Peirce (Peirce, 1937). A purely geometrical model, which involves no consideration of internal forces, is set up by Peirce for the determination of the various parameters that were required. Beyond that, the geometrical structures of knits are another hot research issue, for instances, for plain-knitted fabric structure, Peirce (Peirce, 1947), Leaf and Glaskin (Leaf & Glaskin, 1955), Munden (Munden, 1961), Postle (Postle, 1971), DemirÖz and Dias (Demiröz & Dias, 2000), Kurbak (Kurbak, 1998), Semnani (Semnani et al., 2003), and Chamberlain (Chamberlain, 1949) et al. Lately, Kurbak & Alpyildiz propose a geometrical model for full (Kurbak & Alpyildiz, 2009) and half (Kurbak & Alpyildiz, 2009) cardigan structure. Both the knitted and woven fabrics are considered to be useful as a reinforcing material within composites. The geometrical structure of the plain woven fabric (WF) is considered in this study.

Woven fabric is a two-dimension (2-D) plane formation and represents the basic structural element of every item of clothing. Fabrics are involved to various levels of load in transforming them from 2-D form into 3-D one for an item of clothing. It is important to know the physical characteristics and mechanical properties of woven fabrics to predict possible behavior and eventual problems in clothing production processes. Therefore, the prediction of the elastic properties has received considerable attention. Fabric mechanics is described in mathematical form based on geometry. This philosophy was the main objective of Peirce's research on tensile deformation of weave fabrics. The load-extension behavior of woven fabrics has received attention from many researchers. The methods used to develop the models by the researches are quite varied. Some of the developed models are theory-based on strain-energy relationship e.g., the mode by Hearle and Shanahan (Hearle &

Shanahan, 1978), Grosberg and Kedia (Grosberg & Kedia, 1966), Huang (Huang, 1978), de Jong and Postle (Jong & Postle, 1977), Leaf and Kandil (Leaf & Kandil, 1980), and Womersley (Womersley, 1937). Some of them are based on AI-related technologies that have a rigorous, mathematical foundation, e.g., the model by Hadizadeh, Jeddi, and Tehran (Hadizadeh et al., 2009). Artificial neural network (ANN) is applied to learn some feature parameters of instance samples in training process. After the training process, the ANN model can proceed with the prediction of the load-extension behavior of woven fabrics. The others are based on digital image processing technology, e.g., the model by Hursa, Rotich and Ražić (Hursa et al., 2009). A digital image processing model is developed to discriminate the differences between the image of origin fabric and that of the deformed one after applying loading so as to determine pseudo Poisson's ratio of the woven fabric.

However, the above-mentioned methods have their limitations and shortcomings. The methods based on extension-energy relationship and system equilibrium need to use a computer to solve the basic equations in order to obtain numerical results that can be compared with experimental data. The methods based on AI-related technologies (i.e., ANN model) need to prepare a lot of feature data of samples for the model training before it can work on the prediction. Thus, the developed prediction models need quite a lot of tedious preparing works and large computation.

In this study, a unit cell model based on slice array model (SAM) (Naik & Ganesh, 1992) for plain weave is developed to predict the elastic behavior of a piece of woven fabric during extension. Because the thickness of a fabric is small, a piece of woven fabric can be regarded as a thin lamina. The plain weave fabric lamina model presented in this study is 2-D in the sense that considers the undulation and continuity of the strand in both the warp and weft directions. The model also accounts for the presence of the gap between adjacent yarns and different material and geometrical properties of the warp and weft yarns. This slice array model (i.e., SAM), the unit cell is divided into slices either along or across the loading direction, is applied to predict the mechanical properties of the fabric. Through the help of the prediction model, the mechanic properties (e.g., initial Young's modulus, surface shear modulus and Poisson's ratio) of the woven fabric can be obtained in advance without experimental testing. Before the developed model can be applied to prediction, there are parameters, e.g., the sizes of cross-section of the yarns, the undulation angles of the interlaced yarns, the Young's modulus and the bending rigidity of the yarns, and the unit repeat length of the fabric etc., needed to be obtained. In order to efficiently acquire these essential parameters, an innovative methodology proposed in this study to help eliminate the tedious measuring process for the parameters. Thus, the determination of the elastic properties for the woven fabric can be more efficient and effective through the help of the developed prediction model.

## **2. Innovative evaluation methodology for cross-sectional size of yarn**

### **2.1 Definitions and notation for fundamental magnitudes of fabric surface**

A full discussion of the geometrical model and its application to practical problems of woven fabric design has been given by Peirce (Peirce, 1937). The warp and weft yarns, which are perpendicular straight lines in the ideal form of the cloth, become curved under stress, and form a natural system of curvilinear co-ordinates for the description of its deformed state. The geometrical model of fabric is illustrated in Fig. 1. The basic parameters

consist of two values of yarn lengths  $l$ , two crimp heights,  $h$ , two yarn spacings,  $P$ , and the sum of the diameters of the two yarns,  $D$ , give any four of these, the other three can be calculated from the model. There are three basic relationships as shown in equations 1~3 among these parameters. The definitions of the parameters set in the structural model are denoted as follows.

$$h = (l - D\theta)\sin\theta + D(1 - \cos\theta) \tag{1}$$

$$p = (l - D\theta)\cos\theta + D\sin\theta \tag{2}$$

$$h_w + h_f = D \tag{3}$$

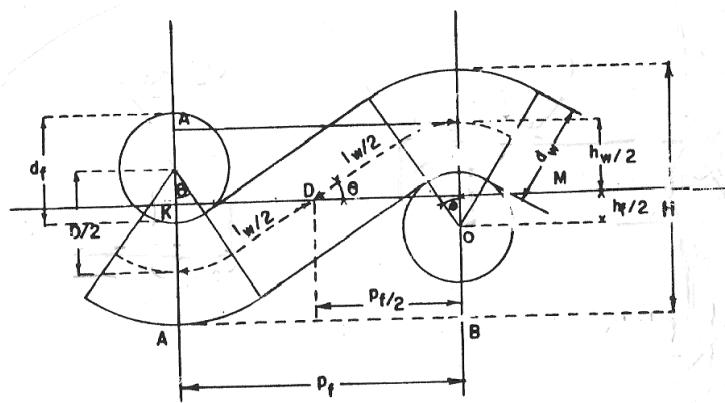


Fig. 1. Geometrical model (Hearle et al., 1969)

- Diameter of warp  $d_w$ , diameter of weft yarn  $d_f$ , and  $d_w + d_f = D$ .
- Distance between central plane of adjacent warp yarns  $P_w$
- Distance between central plane of adjacent weft yarns  $P_f$
- Distance of centers of warp yarns from center-line of fabric,  $h_w/2$
- Distance of centers of weft yarns from center-line of fabric,  $h_f/2$
- Inclination of warp yarns to center-line of fabric,  $\theta_w$
- Inclination of weft yarns to center-line of fabric,  $\theta_f$
- Length of warp between two adjacent weft yarns  $l_w$
- Length of weft between two adjacent warp yarns  $l_f$
- Warp crimp  $C_w = l_w / P_f - 1$
- Weft crimp  $C_f = l_f / P_w - 1$

The woven fabric, which consists of warp and weft yarns interlaced one another, is an anisotropic material (Sun et al., 2005). In order to construct an evaluation model to help determine the size of the deformed shape (i.e., eye shape) of cross section, Peirce's plain weave geometrical structure model is applied in this study. Because both the warp and weft yarns of the woven fabric are subject to the stresses during weaving process by the shedding, picking and beating motions, the shapes of cross section for the yarns are not actually the idealized circular ones (Hearle et al., 1969). The geometrical relations, illustrated in equations 1 and 2, can be obtained by projection in and perpendicular to the plane of the fabric. From these fundamental relations between the constants of the fabrics, the shape and the size of the cross section of the yarns can be acquired. Through the assistance of the

proposed evaluation model, the efficiency and effectiveness in acquiring the size of section for warp (weft) yarn can be improved.

## 2.2 Yarn crimp

The crimp (Lin, 2007)(i.e.,  $C_w$ ) of warp yarn and that (i.e.,  $C_f$ ) of weft yarn can be obtained by using equation 4. The measuring of yarn crimp is performed according to Chinese National Standard (C.N.S.). During measuring the length of the yarn unravelled from sample fabric (i.e., with a size of 20 cm × 20 cm), each yarn was hung with a loading of 346/N (g), where N is the yarn count (840 yds/1lb) of the yarn for testing.

$$C = (L - L') / L' \quad (4)$$

Where L denotes the measured length of the warp (weft) yarn,  $L'$  denotes the length of the fabric in the warp (weft) direction.

## 2.3 Cross sectional shape and size

Both the warp and weft yarns of the woven fabric are subject to the stresses from weaving process during the shedding, picking and beating motions. Due to subjecting to stresses, the shapes of cross section for the yarns are not actually the idealized circular ones. Fig. 2 shows the deformed eye shape of the yarn with a long diameter "a" and a short diameter "h". The sizes of warp and weft yarn are of denoted as  $a_w$ ,  $h_w$  and  $a_f$ ,  $h_f$ , respectively.

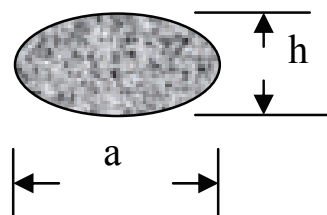


Fig. 2. Deformed shape of yarn

The Length of warp  $l_1$  (weft  $l_2$ ) between two adjacent weft (warp) yarns can be acquired using equation 5. The inclination of warp  $\theta_1$  (weft  $\theta_2$ ) yarns to center-line of fabric, can be obtained from equation 6, which is proposed by Grosberg (Hearle et al., 1969) and verified to be very close to the accurate inclination degree.

$$l = \frac{1 + 1 / 2nC}{N} \quad (5)$$

$$\theta = 106\sqrt{C} \quad (6)$$

where

C: Crimp

n: number of the warp and weft yarns in one weave repeat

N: Weaving density (ends/in; picks/in)

By Putting the measured values of  $l$  and  $\theta$  into equations 1 and 2, the summation of the sizes of the short diameter for the warp and weft yarns (i.e.,  $D = h_w + h_f$  for the warp and weft in the thickness direction) and that of the sizes of the long diameter for the warp and weft yarns (i.e.,  $D_1 = a_w^1 + a_f^1$  ( $D_2 = a_w^2 + a_f^2$ )) calculated from the known distance between central

plane of adjacent warp  $P_w$  (weft  $P_f$ ) yarns). Because the obtained summation values calculated from the known distances between central plane of adjacent warp yarns  $P_w$  and weft yarns  $P_f$  are different, the average value  $\bar{D}$  of them is calculated. The obtained  $\bar{D}$  represents the sum of the long diameters of the warp and weft yarns. The larger the value of  $\bar{D}$  is, the more flattened shape the warp and weft yarns are.

Although the summation for the diameter sizes of the warp and weft yarn in the length (thickness) direction of the woven fabric is obtained, the individual one for warp (weft) yarn is still uncertain. In order to estimate the individual diameters of warp and weft yarn, the theoretical diameter (Lai, 1985) is evaluated using equation 7 in the study. The diameter of the individual yarn can be estimated by the weigh ratios shown in equations 8~11.

$$d (\mu m)=11.89 \sqrt{\frac{\text{Denier}}{\rho}} \quad (7)$$

where

Denier: denier of yarn

$\rho$ : specific gravity of yarn

$$a_w = \bar{D} \times \frac{d_w}{d_w + d_f} \quad (8)$$

$$a_f = \bar{D} \times \frac{d_f}{d_w + d_f} \quad (9)$$

$$h_w = D \times \frac{d_w}{d_w + d_f} \quad (10)$$

$$h_f = D \times \frac{d_f}{d_w + d_f} \quad (11)$$

where

$a_w$ : Long diameter of eye-shaped warp yarn

$a_f$ : Long diameter of eye-shaped weft yarn

$h_w$ : Short diameter of eye-shaped warp yarn

$h_f$ : Short diameter of eye-shaped weft yarn

$D = h_w + h_f$

$\bar{D} = (D_1 + D_2) / 2$

$d_w$ : Theoretical diameter of circular warp yarn

$d_f$ : Theoretical diameter of circular weft yarn

### 3. Geometrical model and properties of spun yarn

The idealized staple fiber yarn is assumed to consist of a very large number of fibers of limited length, uniformly packed in a uniform circular yarn. The fibers are arranged in a helical assembly, following an idealized migration pattern. Each fiber follows a helical path, with a constant number of turns per unit length along the yarn, in which the radial distance



from the yarn axis increases and decreases slowly and regularly between zero and the yarn radius. A fiber bundle illustrated in Fig. 3a, which is twisted along a helical path as shown in Fig. 3b, is manufactured into a twisted spun yarn.

In order to describe the distributed stresses on the body of yarn, a hypothetical rectangular element from is proposed and illustrated in Fig. 4. The stresses acting on the elemental volume  $dV$  are shown in Fig. 4. When the volume  $dV$  shrinks to a point, the stress tensor is represented by placing its components in a  $3 \times 3$  symmetric matrix. However, a six-independent-component is applied as follows.

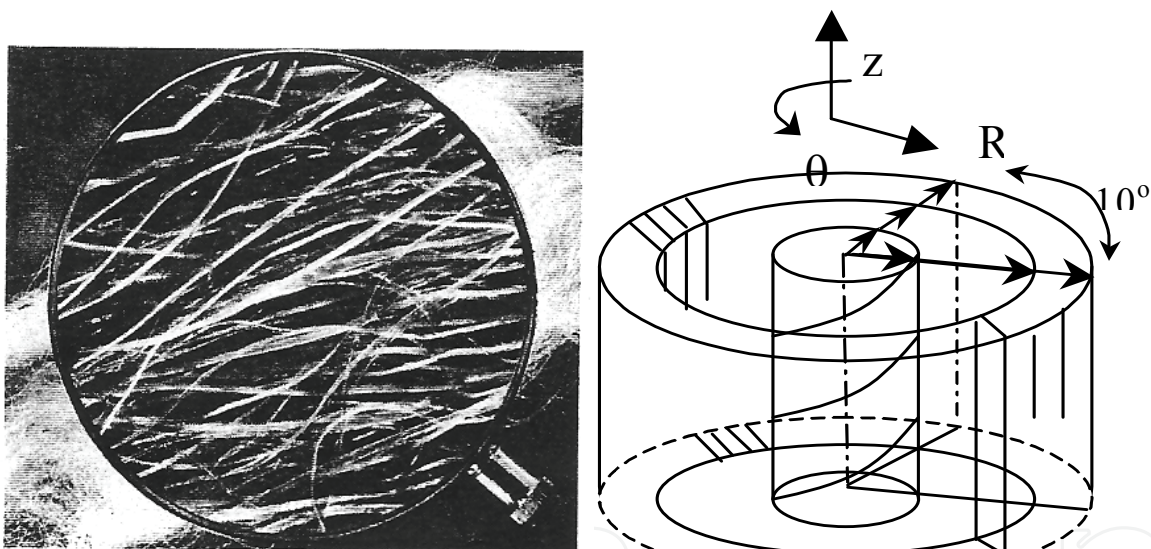
$$\sigma = [\sigma_x, \sigma_y, \sigma_z, \tau_{yz}, \tau_{zx}, \tau_{xy}]^T \quad (12)$$

Where  $\sigma_x, \sigma_y, \sigma_z$  are normal stresses and  $\tau_{yz}, \tau_{zx}, \tau_{xy}$  are shear stresses.

The strains corresponded to the acting stresses can be represented as follows.

$$\varepsilon = [\varepsilon_x, \varepsilon_y, \varepsilon_z, \gamma_{yz}, \gamma_{zx}, \gamma_{xy}]^T \quad (13)$$

Where  $\varepsilon_x, \varepsilon_y, \varepsilon_z$  are normal strains and  $\gamma_{yz}, \gamma_{zx}, \gamma_{xy}$  are engineering shear strains.



(a) A fiber bundle as seen under a magnifying (Curiskis & Carnaby, 1985 ) b) fiber bundle twisted along a helical path

Fig. 3. A fiber bundle

In the continuum mechanics of solids, constitutive relations are used to establish mathematical expressions among the variables that describe the mechanical behavior of a material when subjected to applied load. Thus, these equations define an ideal material response and can be extended for thermal, moisture, and other effects. In the case of a linear elastic material, the constitutive relations may be written in the form of a generalized Hooke's law:

$$\sigma = [S] \varepsilon \quad (14)$$

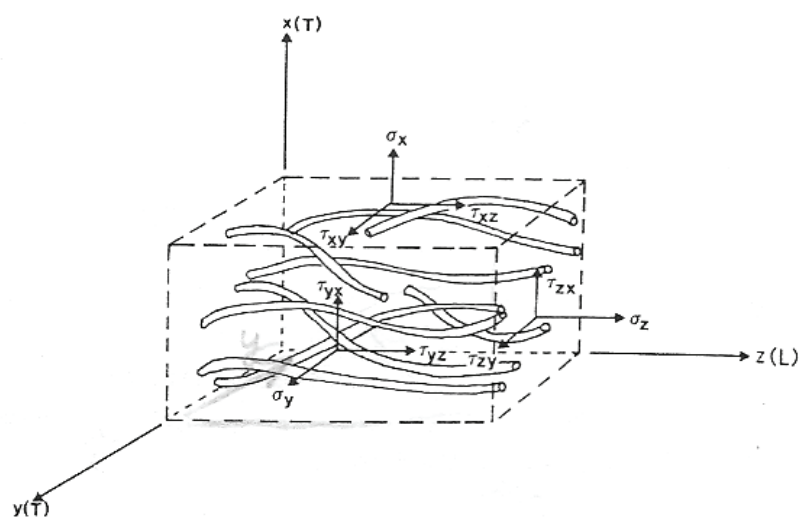


Fig. 4. A rectangular element of a fiber bundle (Curiskis & Carnaby, 1985 )  
That is

$$\begin{Bmatrix} \sigma_x \\ \sigma_y \\ \sigma_z \\ \tau_{xy} \\ \tau_{yz} \\ \tau_{zx} \end{Bmatrix} = \begin{bmatrix} S_{11} & S_{12} & S_{13} & S_{14} & S_{15} & S_{16} \\ S_{21} & S_{22} & S_{23} & S_{24} & S_{25} & S_{26} \\ S_{31} & S_{32} & S_{33} & S_{34} & S_{35} & S_{36} \\ S_{41} & S_{42} & S_{43} & S_{44} & S_{45} & S_{46} \\ S_{51} & S_{52} & S_{53} & S_{54} & S_{55} & S_{56} \\ S_{61} & S_{62} & S_{63} & S_{64} & S_{65} & S_{66} \end{bmatrix} \begin{Bmatrix} \varepsilon_x \\ \varepsilon_y \\ \varepsilon_z \\ \gamma_{xy} \\ \gamma_{yz} \\ \gamma_{zx} \end{Bmatrix} \tag{15}$$

$$\varepsilon = [C]\sigma \tag{16}$$

That is

$$\begin{Bmatrix} \varepsilon_x \\ \varepsilon_y \\ \varepsilon_z \\ \gamma_{xy} \\ \gamma_{yz} \\ \gamma_{zx} \end{Bmatrix} = \begin{bmatrix} C_{11} & C_{12} & C_{13} & C_{14} & C_{15} & C_{16} \\ C_{21} & C_{22} & C_{23} & C_{24} & C_{25} & C_{26} \\ C_{31} & C_{32} & C_{33} & C_{34} & C_{35} & C_{36} \\ C_{41} & C_{42} & C_{43} & C_{44} & C_{45} & C_{46} \\ C_{51} & C_{52} & C_{53} & C_{54} & C_{55} & C_{56} \\ C_{61} & C_{62} & C_{63} & C_{64} & C_{65} & C_{66} \end{bmatrix} \begin{Bmatrix} \sigma_x \\ \sigma_y \\ \sigma_z \\ \tau_{xy} \\ \tau_{yz} \\ \tau_{zx} \end{Bmatrix} \tag{17}$$

Where  $\sigma$  and  $\varepsilon$  are suitably defined stress and strain vectors (Carnaby 1976) (Lekhnitskii , 1963), respectively, and  $[S]$  and  $[C]$  are stiffness and compliance matrices, respectively, reflecting the elastic mechanical properties of the material (i.e., moduli, Poission’s ratios, etc.) There are four possible models (Curiskis & Carnaby, 1985) (Carnaby & Luijk, 1982) for the continuous fiber bundle, i.e., the general fiber bundle, Orthotropic material, square-symmetric material, and transversely isotropic material. The orthotropic material model is adopted in this study.

Thwaites (Thwaites, 1980) applied his equations subject to the further constrain of incompressibility of the continuum, that is,



$$\varepsilon_x + \varepsilon_y + \varepsilon_z = 0 \quad (18)$$

In which case the two Poisson's ratio terms are no longer independent :

$$G_{TT} = \frac{E_T}{2(1 + v_{TT})} \quad (19)$$

$$v_{TT} = 1 - v_{TL} \quad (20)$$

And

$$v_{TL} = v_{LT} E_T / E_L \quad (21)$$

Thus, for the incompressible material of a spun yarn, whose elastic properties can be described using the seven elastic constants, i.e.,  $G_{TT}$ ,  $G_{LT}$ ,  $E_T$ ,  $E_L$ ,  $v_{LT}$ ,  $v_{TL}$ , and  $v_{TT}$ , an orthotropic material model is adopted to depict it in this study. The orthotropic material model as shown in Fig. 4, the fiber packing in the xy plane and along the z axis is such that the xz and yz planes are also planes of elastic symmetry. Furthermore, the continuum idealization then allows application of the various mathematical techniques of continuum mechanics to simplify the setting-up of physical problems in order to obtain useful results for various practical situations. For the study, the yarn (fiber bundle) is mechanically characterized as a degenerate square-symmetric homogeneous continuum. The elastic compliance relationship (Carnaby, 1980) can be described using the moduli and Poisson's ratio parameters illustrated as follows.

$$\begin{Bmatrix} \varepsilon_x \\ \varepsilon_y \\ \varepsilon_z \\ \gamma_{xy} \\ \gamma_{yz} \\ \gamma_{zx} \end{Bmatrix} = \begin{bmatrix} \frac{1}{E_T} & -\frac{V_{TT}}{E_T} & -\frac{V_{LT}}{E_L} & 0 & 0 & 0 \\ -\frac{V_{TT}}{E_T} & \frac{1}{E_T} & -\frac{V_{LT}}{E_L} & 0 & 0 & 0 \\ -\frac{V_{TL}}{E_T} & -\frac{V_{TL}}{E_T} & \frac{1}{E_L} & 0 & 0 & 0 \\ 0 & 0 & 0 & \frac{1}{G_{TT}} & 0 & 0 \\ 0 & 0 & 0 & 0 & \frac{1}{G_{LT}} & 0 \\ 0 & 0 & 0 & 0 & 0 & \frac{1}{G_{LT}} \end{bmatrix} \begin{Bmatrix} \sigma_x \\ \sigma_y \\ \sigma_z \\ \gamma_{xy} \\ \gamma_{yz} \\ \gamma_{zx} \end{Bmatrix} \quad (22)$$

Where  $E_L$  is the longitudinal modulus governing uniaxial loading in the longitudinal (z) direction.  $v_{LT}$  is the associated Poisson ratio governing induced transverse strains,  $E_T$  is the transverse modulus governing uniaxial loading in the transverse (x or y) direction.  $v_{TT}$  is the associated Poisson ratio governing resultant strains in the remaining orthogonal transverse (y or x) direction.  $v_{TT}$  is the associated Poisson ratio governing the induced strain in the longitudinal direction,  $G_{LT}$  is the longitudinal shear modulus governing shear in the longitudinal direction, and  $G_{TT}$  is the transverse shear modulus governing shear in the transverse plane.

The theoretical equation for Young's modulus of the spun yarn developed by Hearle (Hearle et al., 1969) is adopted in the study. It is illustrated in equation 23. The fibers are assumed to have identical dimensions and properties, to be perfectly elastic, to have an axis of symmetry, and to follow Hooke's and Amonton's laws. The strains involved are assumed to be small. The transverse stresses between the fibers at any point are assumed to be the same in all directions perpendicular to the fiber axis. Beyond these, there are other assumptions for the developed equation. Thus, it can not expected to be numerically precise because of the severe approximations, can be expected to indicate the general form of the factors affecting staple fiber yarn modulus. However, despite the differences between the idealized model and actual yarns, it is useful to have a knowledge of how an idealized assembly would behave.

$$Y_M = f_M \times \frac{1 - \frac{2}{3L_f} \left\{ \frac{a\gamma W_y^{1/2} (1 + 4\pi v_f \phi^{-1} \tau^2 10^{-5})^{1/2}}{4\tau\mu [1 - (1 + 4\pi v_f \phi^{-1} \tau^2 10^{-5})^{-1/2}]} \right\}^{1/2}}{(1 + 4\pi v_f \phi^{-1} \tau^2 10^{-5})} \quad (23)$$

Where

$f_M$ : modulus of fiber

$L_f$ : fiber length

$a$ : fiber radius

$\gamma$ : migration ratio ( $\gamma=4$  for spun yarn)

$W_y$ : yarn count (tex)

$v_f$ : specific volume of fiber

$\phi$ : packing fraction

$\tau$ : twist factor ( $\text{tex}^{1/2}$  turn/cm)

$\mu$ : coefficient of friction of fiber

The flexural rigidity of a filament yarns is the sum of the fiber flexural rigidities under the circumstance that the bending length of the yarn is equal to that of a single fiber. It has been confirmed experimentally by Carlen (Hearle et al., 1969) (Cooper, 1960). The spun yarn is regarded as a continuum fiber bundle in the study, so the flexural rigidity of it is approximately using the same prediction equation illustrated in equation 24.

$$G_y = N_f G_f \quad (24)$$

Where

$N_f$ : cross-sectional fiber number

$G_f$ : flexure rigidity of fiber

The change of yarn diameter and volume with extension has been investigated by Hearle etc. (Hearle et al., 1969) Through the experimental results for the percentage reductions in yarn diameter with yarn extension by Hearle, the Poisson's ratio  $\nu_{LT}$  in the extension direction can be estimated to be at the range of 0.6 ~ 1.1. The Poisson's ratio  $\nu_{LT}$  is set to be 0.7 for the spun yarn in the study.

Young's modulus  $E_L$  of the yarn in the (length) extension direction can be estimated using equation 23. Equation 24 can be applied to estimate the flexure rigidity  $G_{TL}$  of the yarn. Through putting the obtained  $E_L$ ,  $G_{TL}$ , and the set value of 0.7 for the Poisson's ratio  $\nu_{LT}$  of the yarn into equations 19~21, the other four elastic properties (i.e.,  $G_{TT}$ ,  $E_T$ ,  $\nu_{TL}$ ,  $\nu_{TT}$ ) can be acquired, respectively.

Now that the elastic properties of a spun yarn can be represented using the above-mentioned matrix. The simplification for the setting-up of physical problems using various mathematical techniques of continuum mechanics can thus be achieved. For the study, the yarn (fiber bundle) is mechanically characterized as a degenerate square-symmetric homogeneous continuum. The complex mechanic properties of the combination of the warp and weft yarns interlaced in woven fabric can be possible to be constructed as follows.

#### 4. Construction of unit cell model

##### 4.1 Mechanical properties of unit cell of fabric

Fig.5a illustrates a unit cell (Naik & Ganesh, 1992) of woven fabric lamina. There is only one quarter of the interlacing region analysed due to the symmetry of the interlacing region in plain weave fabric.

The analysis of the unit cell, i.e., slice array model (SAM), is performed by dividing the unit cell into a number of slices as illustrated in Fig. 5b. The sliced pieces are idealized in the form of a four-layered laminate, i.e., an asymmetric crossply sandwiched between two pure matrix (if any) layers as shown in Fig. 5c. The effective properties of the individual layer considering the presence of undulation are used to evaluate the elastical constants of the idealized laminate. Because there is no matrix applied, the top and the bottom layer of the unit cell are not included in this study.

There are two shape functions proposed in the study, one as shown in Fig. 6a for the cross-section in the warp direction and the other as illustrated in Fig. 6b for the one in the weft direction.

Along the warp direction, i.e., in the Y-Z plane (Fig. 5(a))

$$z_{y1}(y) = -\frac{h_f}{2} \cos \frac{\pi y}{a_{yt}} \quad (25)$$

$$z_{y2}(y) = \frac{h_f}{2} \cos \frac{\pi y}{a_f + g_f} \quad (26)$$

Where

$$a_{yt} = \frac{\pi a_f}{2 \left[ \pi - \cos^{-1} \left( \frac{2z_{yt}}{h_f} \right) \right]}, \quad z_{yt} = \frac{h_f}{2} \cos \frac{\pi a_f}{2(a_f + g_f)}$$

and

$$\left. \begin{aligned} hy_1(y) &= \frac{h_f + h_m}{2} - zy_2(y) \\ hy_2(y) &= h_w \\ hy_3(y) &= zy_2(y) - zy_1(y) \text{ (when } y = 0 \rightarrow a_f / 2) \\ &= 0 \text{ (when } y = a_f / 2 \rightarrow (a_f + g_f) / 2) \\ hy_4(y) &= \frac{h_f + h_m}{2} - zy_1(y) \end{aligned} \right\} \quad (27)$$

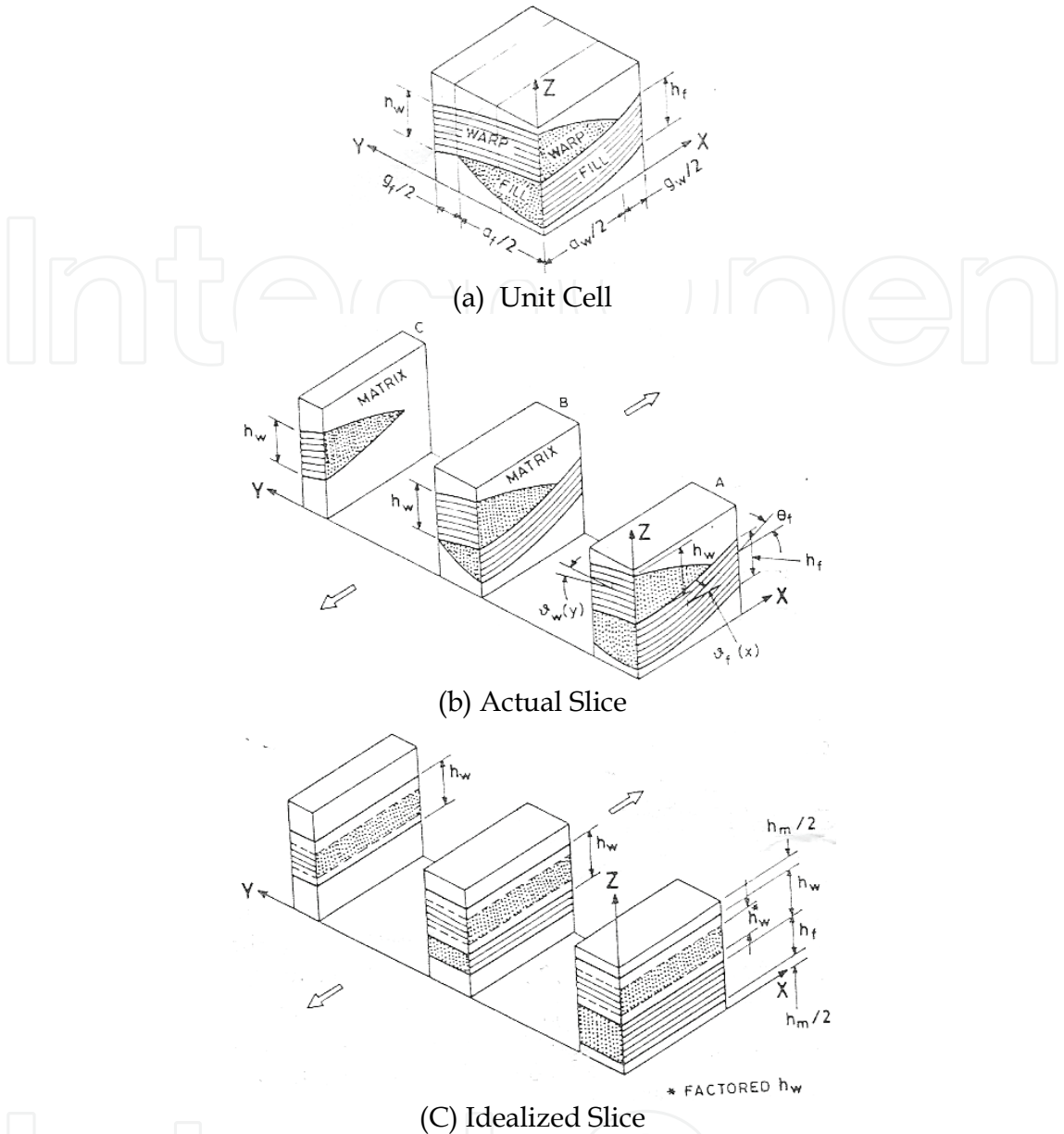


Fig. 5. Illustration for the slicing of unit cell and the idealized slice (Naik & Ganesh, 1992)  
Along the weft (fill) direction, i.e., in the X-Z plane (Fig. 5(a))

$$zx_{1_1}(x,y)=\frac{h_w}{2}\cos\frac{\pi x}{a_{xt}}-hy_1(y)+\frac{h_m}{2}\tag{28}$$

$$zx_2(x,y)=-\frac{h_w}{2}\cos\frac{\pi x}{a_w+g_w}-hy_1(y)+\frac{h_m}{2}\tag{29}$$

where

$$a_{xt}=\frac{\pi a_w}{2\cos^{-1}\left(\frac{2z_{xt}}{h_w}\right)},\; z_{xt}=-\frac{h_w}{2}\cos\frac{\pi a_w}{2(a_w+g_w)};$$

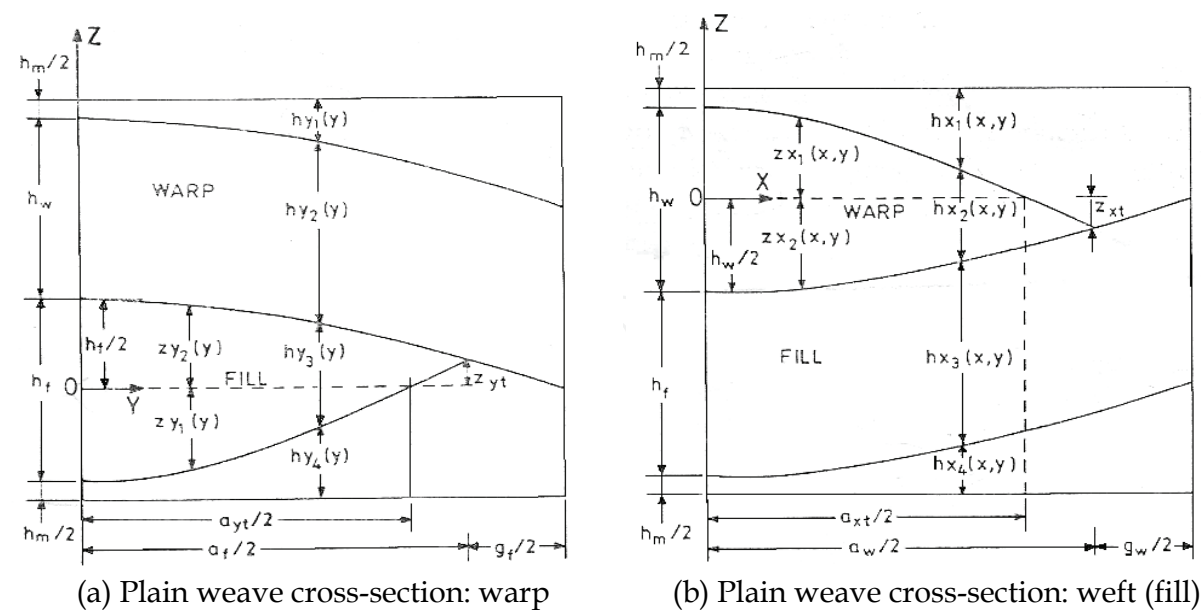


Fig. 6. Illustration for the shape functions (Naik & Ganesh, 1992)

And

$$\left. \begin{aligned} hx_1(x,y) &= \frac{h_w + h_m}{2} - zx_1(x,y) \\ hx_2(x,y) &= zx_1(x,y) - zx_2(x,y) \text{ (when } x = 0 \rightarrow a_w / 2) \\ &= 0 \text{ (when } x = a_w / 2 \rightarrow (a_w + g_w) / 2) \\ hx_3(x,y) &= hy_3(y) \\ hx_4(x,y) &= zx_2(x,y) - hx_3(x,y) + (h_w + h_m) / 2 + h_f \end{aligned} \right\} \tag{30}$$

The local off-axis angles in the weft (i.e.,fill) and warp direction can be calculated using equations 31 and 32, respectively.

$$\theta_f(x) = \tan^{-1} \frac{d}{dx} [zx_2(x,y)] = \tan^{-1} \left( \frac{\pi h_w}{2(a_w + g_w)} \sin \frac{\pi x}{(a_w + g_w)} \right) \tag{31}$$

$$\theta_w(y) = \tan^{-1} \frac{d}{dy} [zy_2(y)] = \tan^{-1} \left( \frac{\pi h_f}{2(a_f + g_f)} \sin \frac{\pi y}{(a_f + g_f)} \right) \tag{32}$$

Because the woven fabric is manufactured by the interlacing of warp and weft yarn, there exists a certain amount of gap between two adjacent yarns. It is obvious that the presence of a gap between two the adjacent yarns would affect the stiffness of the WF lamina. Furthermore, the warp and weft yarns interlaced in fabric are undulated. It can be expected that the elastic properties of the yarn under the straight form and the undulated one are definitely different.

4.2 Mechanical properties of the undulated spun yarn

The respective off-axis angles reduce the effective elastic constants in the global X and Y directions. The increased compliance can be evatuated as follows. (Lekhnitskii, 1963).

$$C_{11}(\vartheta) = \frac{1}{E_L(\vartheta)} = \frac{m^4}{E_L} + \left(-\frac{1}{G_{LT}} + \frac{2v_{LT}}{E_L}\right)m^2n^2 + \frac{n^4}{E_T} \quad (33)$$

$$C_{22}(\vartheta) = \frac{1}{E_T(\vartheta)} = \frac{1}{E_T} \quad (34)$$

$$C_{12}(\vartheta) = \frac{v_{TL}(\vartheta)}{E_T(\vartheta)} = \frac{v_{TL}m^2}{E_T} + \frac{v_{TT}n^2}{E_T} \quad (35)$$

$$C_{66}(\vartheta) = \frac{1}{G_{LT}(\vartheta)} = \frac{m^2}{G_{LT}} + \frac{n^2}{G_{TT}} \quad (36)$$

Where  $m = \cos \vartheta$ ,  $n = \sin \vartheta$ ;  $E_L$  and  $E_T$  are Young's moduli of yarns in the length direction and the cross-sectional direction, respectively;  $G_{LT}$  and  $G_{TT}$  are the flexure rigidity and torsion one, respectively. The value of  $E_L$  is calculated by the theoretical equation 23 developed by Hearle (Hearle et al., 1969). Through the experimental results for the percentage reductions in yarn diameter with yarn extension by Hearle, the values of  $E_T$ ,  $G_{LT}$ , and  $G_{TT}$  for the yarns are determined based on the orthotropic material model proposed by Curiskis and Carnaby (Curiskis & Carnaby, 1985).

The compliance of yarn is related to the angle of undulation of the yarn crimped in the fabric. The off-axis angle for each specific location at the warp and weft yarn can be acquired from equation 31 and 32. In order to precisely evaluate the changed compliances for the warp and weft yarn, the mean value of the compliance is applied and illustrated in equation 37.

$$\bar{C}_{ij} = \frac{1}{\theta} \int_0^\theta C_{ij}(\vartheta) d\vartheta \quad (37)$$

where  $\theta$  is the angle of undulation for the yarn at  $x=a_w/2+g_w/2$ .

#### 4.3 Evaluation of mechanical properties of slices and unit cell

After evaluating the changed elastic constants of the warp and weft yarn using equation 37, the extensional stiffness of the slice can be obtained from equation 38. The integration used in the equation is fulfilled by neumatic method in the study.

$$A_{ij}^{sl}(y) = \frac{1}{H} \sum_{k=1}^2 hx_k(x, y) (\bar{S}_{ij})_k \quad (38)$$

Where,  $hx_k(x, y)$  and  $(\bar{S}_{ij})_k$  are the thickness and mean transformed stiffness of the  $k$ th layer in the  $n$ th slice.

The sliced pieces are idealized in the form of a two-layered lamina, i.e., warp and weft asymmetric crossply sandwiched between two pure matrix (if any) layers as shown in Fig. 5c. If there is no matrix applied on the fabric, i.e., the 1st and the 4th layers are vacant; the extensional stiffness of the slice consisting of a warp and a weft yarn can still be estimated from equation 38. The effective properties of the individual layer considering the presence of undulation are used to evaluate the elastical constants of the idealized woven fabric lamina.



Based on Fig. 5 and Fig. 6,  $h_{x_k}(x,y)$  is evaluated at constant  $x$ , for different values of  $y$ . The thickness of the warp yarn is maximum at  $x=0$  and zero from  $x=a_w/2$  to  $x=(a_w+g_w)/2$ . In order to acquire the mean thickness of each layer of different material, the coordinate of  $x$  is set to be at the middle (i.e.,  $x= (a_w/2+g_w/2)/2$ ) of the unit cell in the study. The extensional stiffness of the unit cell is evaluated from those of the slices by assembling the slices together under the isostrain condition in all the slices. In other words, the in-plane extensional stiffness of the unit cell is evaluated and can be expressed as follows.

$$A_{ij} = \frac{2}{(a_f + g_f)} \int_0^{(a_f+g_f)/2} A_{ij}^s(y) dy$$

(39)

According to Fig. 5a, the unit cell is obviously not symmetric about its midplane, so there exist the coupling stiffness terms. However, the coupling terms in two adjacent unit cells of the woven fabric lamina would be opposite signs due to the nature of interlacing of yarns in the plain weave fabric. Thus, the elastic constants of the unit can be obtained and expressed as follows.

$$\left. \begin{aligned} E_x &= A_{11} \left( 1 - \frac{A_{12}^2}{A_{11} A_{22}} \right) \\ G_{xy} &= A_{66} \\ \nu_{yx} &= \frac{A_{12}}{A_{22}} \end{aligned} \right\}$$

(40)

Where,  $E_x$  is the Young’s modulus,  $G_{xy}$  is the flexure rigidity, and  $\nu_{yx}$  is the Poisson’s ratio for the fabric, respectively. Accordingly, the Young’s modulus in the warp direction can be calculated using the above-mentioned steps as well.

5. Experiments

5.1 Characteristics of sample fabrics

The measured characteristics of the sample fabric are shown in table 1. The theoretically generalized elastic properties of cotton fiber are given in Table 2. Base on the data of the raw material cotton fiber, Young’s modulus of the cotton spun yarn (i.e.,  $y_M$ ) is predicted to be 6694 (N/mm<sup>2</sup>) using equation 23 developed by Hearle (Hearle et al., 1969). The flexure rigidity (i.e.,  $G_{LT}$ ) of the spun yarn can be acquired as 0.0031 (N/mm<sup>2</sup>) using equation 24 as well.

Weave	Yarn count (warp×weft)	Yarn specific volume, cm <sup>3</sup> /g	Density, yarns/inch (warp×weft)	Material (warp×weft)
plain	20’S × 20’S	1.22	60 × 60	C × C

Yarn count ‘S=840 yd/ 1lb, Material: C=cotton

Table 1. Characteristics of woven fabric sample

5.2 Preprocessing and procedures

The sample fabrics are scoured at 30°C for one hour in sodium carbonate. Then they are washed and dried at room temperature. Static tensile test specimens are prepared according

to Chinese National Standard (C.N.S.). The testing size is 25mm×100mm. The specimens are tested at room temperature (25°C) at a crosshead speed of 10 mm/min. A total of ten specimens are tested, five of which are the samples made for testing in warp direction and the other five are for testing in weft direction direction. An experimental program is designed by C language to calculate the elastic constants of the woven fabric lamina along the warp and weft directions in the study. The experiment is performed on cotton woven fabric lamina according to the essential requirements proposed by Bassett et al. (Bassett et al., 1999).

$f_M$ (N/mm <sup>2</sup> )	$L_f$ (mm)	$a$ (mm)	$\gamma$	$W_y$ (tex)	$v_f$	$\phi$	$\tau$ (tex <sup>1/2</sup> turns/cm)	$\mu$	$E_L$ (N/mm <sup>2</sup> )	$G_{LT}$ (Nmm <sup>2</sup> )
8000	40	0.0130	4	31.9200	0.6500	0.5300	33.36	0.22	6694	0.0031

$f_M$ : Young’s modulus of fiber,  $L_f$ : fiber length,  $a$ : fiber radius,  $\gamma$ :migration ratio,  $W_y$ : yarn count,  $v_f$ : specific volume of fiber,  $\phi$ :packing fraction,  $\tau$ :twist factor(tex<sup>1/2</sup>turn/cm),  $\mu$ :coefficient of friction

Table 2. Characteristics of the cotton fiber

6. Results and discussion

6.1 Cross-sectional size of yarn

Woven fabric, which consists of warp and weft yarns interlaced one another, is an anisotropic material. Peirce’s plain weave geometrical structure model is used to set up a prediction model for the shapes and sizes of warp and weft yarn. Both the warp and weft yarns of woven fabric are subject to the stresses from weaving process during the shedding, picking, beating motions. Due to the occurred stresses, the shapes of section for yarns are not actually the idealized circular ones. It shows that the theoretically calculated results are pretty consistent to the experimental. Through the evaluation methodology for cross-sectional size of yarn based on Peirce’s structure model, the efficiency and effectiveness in acquiring the sectional size for warp (weft) yarn can be improved.

The geometrical scales of the fabric are determined by means of an optical microscope at a magnification of 20. The obtained results are used to compare with the calculated ones for validation of the innovative evaluation methodology proposed in this study. The measured and calculated results are illustrated in Table 3 and Table 4, respectively. Table 5 shows there are errors less than 5% for each between the calculated and the tested results. It reveals that the proposed method is of good accuracy and can more efficiently acquire the geometrical sizes, i.e., the long and short diameters of the warp and weft yarns in the fabrics.

Crimp		Undulation angle (degree)		Length of repeat unit (mm)		Crimped length (mm)	
$C_w$	$C_f$	$\theta_w$	$\theta_f$	$P_w$	$P_f$	$l_w$	$l_f$
0.06	0.06	25.9646	25.9646	0.4305	0.4305	0.4487	0.4487

Table 3. Measured and induced results of the basic sizes for the fabric

Long diameter		Short diameter	Diameter		Diameter			
$p = (l - D \theta) \cos \theta + D \sin \theta$		$h = (l - D \theta) \sin \theta + D(1 - \cos \theta)$	(circular shape)		(actual eye shape)			
			warp	weft	warp	weft		
$D_1(\text{mm})$	$D_2(\text{mm})$	$D(\text{mm})$	$d_w(\text{mm})$	$d_f(\text{mm})$	$a_w(\text{mm})$	$h_w(\text{mm})$	$a_f(\text{mm})$	$h_f(\text{mm})$
0.8856	0.8856							
$\overline{D}(\text{mm})$		0.3288	0.2140	0.2140	0.4428	0.1644	0.4428	0.1644
0.8856								

Table 4. Calculated results by evaluation methodology based on Peirce’s model

Predicted				Measured			
warp		weft		warp		weft	
$a_w(\text{mm})$	$h_w(\text{mm})$	$a_f(\text{mm})$	$h_f(\text{mm})$	$a_w(\text{mm})$	$h_w(\text{mm})$	$a_f(\text{mm})$	$h_f(\text{mm})$
0.4428	0.1644	0.4428	0.1644	0.4348	0.1625	0.4348	0.1625

Table 5. Comparison between the predicted and the measured sizes

6.2 Extensional behavior of fabric

The generalized load-extension curve as illustrated in Fig. 7 (Hearle et al., 1969) shows three actions, as in the initial decrimping region the load-extension curve possesses a point of inflexion. The initial high modulus of the fabric is probably due to frictional resistance to bending of the thread. Once the frictional restraint is overcome, a relatively low modulus is obtained which is mainly governed by the force needed to unbend the threads in the direction in which the force is being applied, and at the same time, the need to increase the curvature in the threads at the right angles to the direction of application of the force. As the crimp is decreased the size of this force rises very steeply and, as a result, the fibers themselves begin to be extended and in the final region, the load-extension properties of the cloth are almost entirely governed by the load-extension properties of the yarns themselves. According to the description of the load-extension process, it can be concluded that the initial modulus of the fabric is determined by the first part. In other words, the resistance to bending of the thread (including frictional forces affected by the surface features of the warp (weft) yarns and the bending rigidity of the warp (weft) yarns) governs the initial modulus.

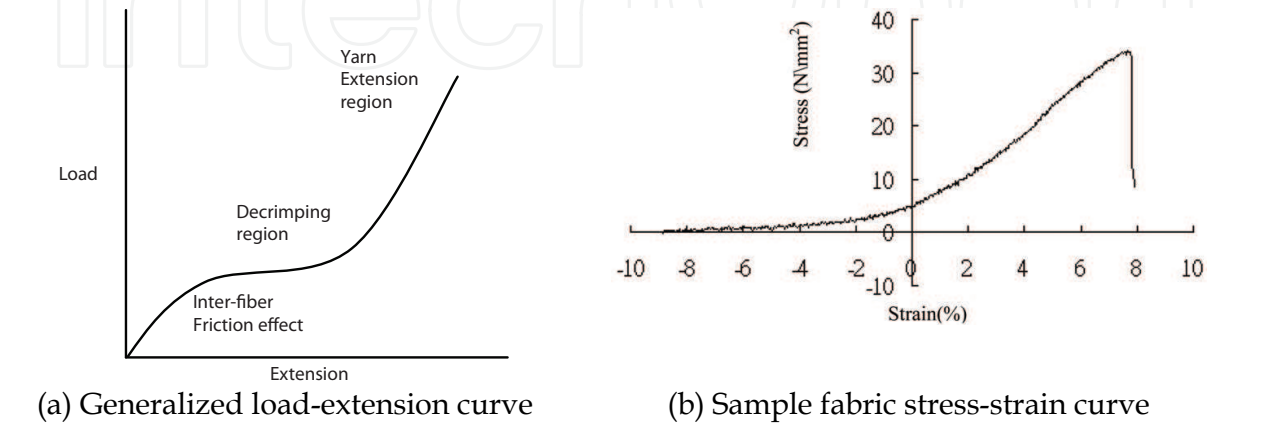


Fig. 7. Comparison between generalized and tested curve

This above-mentioned viewpoints on extension-load curve by Grosberg is quite in accordance with the equation deduced for Young’s modulus by Leaf & Kandil (Leaf & Kandil, 1980). According to the deduced equation, the initial modulus is related to the bending rigidities of warp and weft yarns. However, the tested results for the sample fabric shown in Fig. 7b, in which there is a lack of level out appearance in the load-extension curve for the sample fabric, are different from the generalized load-extension curve. This is mainly because the sample fabric used in the study is of a small crimped angle of 26°. It brings about that once the resistances of the friction force occurred from the rough contact surfaces of the adjacent yarns and the bending rigidities of the warp and weft yarns are conquered, the second stage (i.e., lever out region) is skipped and directly move to the third region (i.e., the applied force used to extend the fibers themselves in the yarn).

6.3 Validation of slice array model

The slice array model (i.e., SAM) (Naik & Ganesh, 1992), which considers the actual yarn cross-sectional geometry and the presence of a gap between the adjant yarns, is presented for the elastic analysis of 2-D orthogonal plain weave fabric lamina. The shape functions agree well with the actual geometry of the woven fabric lamina. The assumption that the locally bending deformations are constrained is realistic considering the nature of interlacing of the plain weave fabrics.

In order to examine the micromechanical approaches for the prediction of the elastic constants of a woven fabric lamina, a plain woven fabric with warp and weft spun yarn of cotton fibers is selected. The elastic properties of the cotton fiber are given in Table 1. Based on the mechanical properties of the raw material cotton fiber, Young’s modulus of the cotton spun yarn (i.e.,  $y_M$ ) is predicted to be 6694 (N/mm<sup>2</sup>) using equation 23 developed by Hearle (Hearle et al., 1969). However, it is much higher than the actual measured value of 581 (N/mm<sup>2</sup>). As Hearle (Hearle et al, 1969) said the prediction equation can not be expected to be numerically precise because of severe approximations.

$E_T$ (N/mm <sup>2</sup> )	$G_{TT}$ (N/mm <sup>2</sup> )	$G_{LT}$ (N/mm <sup>2</sup> )	$\nu_{LT}$	$\nu_{TT}$	$\nu_{TL}$
5592 <sup>a</sup>	1969 <sup>a</sup>	0.0031 <sup>a</sup>	0.70 <sup>a</sup>	0.42 <sup>a</sup>	0.58 <sup>a</sup>
484 <sup>b</sup>	171 <sup>b</sup>	0.0031 <sup>b</sup>	0.70 <sup>b</sup>	0.42 <sup>b</sup>	0.58 <sup>b</sup>

a: Calculated based on  $E_L=6694$  (N/mm<sup>2</sup>); b: Calculated based on  $E_L=581$  (N/mm<sup>2</sup>)

Table 6. Calculated elastic properties of the straight yarn based on Predicted and Measured  $E_L$

$E_x$ (N/mm <sup>2</sup> )	$G_{xy}$ (N/mm <sup>2</sup> )	$\nu_{yx}$
3622 <sup>a</sup>	669 <sup>a</sup>	$1.95 \times 10^{-5}$ <sup>a</sup>
316 <sup>b</sup>	58 <sup>b</sup>	$2.11 \times 10^{-4}$ <sup>b</sup>
363 <sup>c</sup>	---	---

a: Calculated based on  $E_L=6694$  (N/mm<sup>2</sup>); b: Calculated based on  $E_L=581$  (N/mm<sup>2</sup>); c: measured

Table 7. Elastic properties of plain weave fabric lamina: Comparison of predicted and experimental results

Once the value of  $E_L$  is determined and the value of  $\nu_{LT}$  is set at 0.7, those of  $E_T$ ,  $G_{LT}$  and  $G_{TT}$  for the yarns can be calculated based on the orthotropic material model (Curiskis &

Carnaby, 1985) proposed by Curiskis and Carnaby. The obtained results of the mechanical properties of the yarn in straight form are illustrated in Table 6. Thus, the elastic properties (i.e. compliance coefficients) for the undulated warp and weft yarn in the fabric can be estimated by equations 33~36. The compliance matrix for each slice of the unit cell shown in Fig. 5b can thus be obtained and the one of the unit cell can be acquired from the summation of each of the slices as shown in Fig. 5c by equation 39. Furthermore, the stiffness matrix of the unit cell can be calculated from the inverse matrix of the obtained compliance matrix. Young's modulus of the woven fabric in the extension direction can be evaluated using equation 40. The predicted results are illustrated in Table 7, in which it reveals that the predicted Young's modulus  $E_x$  in the weft extension direction based on the actual measured  $E_L$  ( $= 581 \text{ N/mm}^2$ ) of yarn is much closer to the measured one than based on the predicted  $E_L$  ( $=6694 \text{ N/mm}^2$ ) of yarn.

## 7. Conclusions

In this study, a unit cell model for plain weave is developed to predict the elastic behavior of woven fabric during extension. A piece of woven fabric is regarded as a thin lamina because of its thickness is small. The plain weave fabric lamina model presented in this study is 2-D in the sense that considers the undulation and continuity of the strand in both the warp and weft directions. The model also accounts for the presence of the gap between adjacent yarns and different material and geometrical properties of the warp and weft yarns. This slice array model (i.e., SAM), which is used to predict the elastic properties of WF composites by Naik and Ganesh, is applied to evaluate the mechanical properties of woven fabric in this study. The applicability of SAM to prediction of the elastic properties of fabrics is as good as to that of the composites. However, it is necessary to have accurate elastic constants, i.e., Young's moduli of the warp and weft yarn, for the model in order to obtain a promising predicted result. It is found that the accuracy of a predicted Young's moduli of warp and weft yarn obtained from a deduced equation by Hearle is not as good as expected. In order to help eliminate the tedious measuring process but to obtain the exact sizes of the yarns in the fabric, an innovative methodology based on Peirce's geometrical model is developed in the study. It reveals that the proposed method is of good accuracy and can more efficiently acquire the geometrical sizes, i.e., the long and short diameters of the warp and weft yarns in the fabrics. Through the help of the modified SAM prediction model, the mechanic properties (e.g., initial Young's modulus, surface shear modulus and Poisson's ratio) of the woven fabric can be obtained in advance without being through experimental testing. Thus, the determination of the woven fabric can be more efficient and effective through the help of the modified SAM model. Another weave structure of woven fabrics, e.g., twill and satin, is to be selected to construct the geometrical model and a close examination into the stress-strain relations of the unit cell by using finite element analysis is interesting to be followed in our further study.

## 8. References

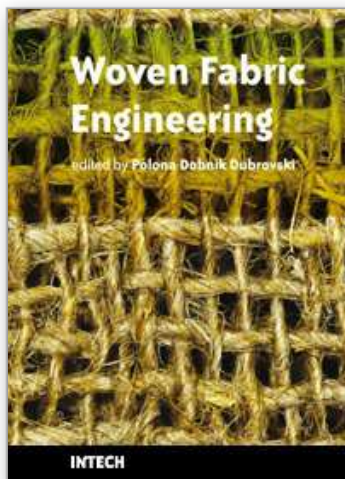
- Bassett, R.J., Postle, R. & Pan, N. (1999). Experimental Methods for Measuring Fabric Mechanical Properties: A Review and Analysis, *Textile Research Journal*, Vol.69, No.11, pp. 866-875



- Curiskis, J.I., Carnaby, G. A. (1985). Continuum Mechanics of the Fiber Bundle, Textile Research Journal, Vol.55, 334-344
- Carlene, P.W. (1950). The Relation between Fiber and Yarn Flexural Rigidity in Continuous Filament Viscose Yarn, The Journal of The Textile Institute, Vol.41, T159-172.
- Cooper, D.N.E. (1960). The Stiffness of Woven Textiles, The Journal of The Textile Institute, Vol.51, T317-335.
- Carnaby, G. A. (1980). The Compression of Fibrous Assemblies, with Applications to Yarn Mechanics, in "Mechanics of Flexible Fiber Assemblies," J.W.S. Hearle, J.J. Thwaites, and J. Amirbayat, Eds., Sijthoff and Noordhoff, Alphen aan den Rijn, The Netherlands, , pp. 99-112.
- Carnaby, G.A. & Luijk, C.J. Van (1982). The Mechanical Properties of Wool Yarns, in "Objective Specification of Fabric Quality, Mechanical Properties and Performance, S.Kawabata, R. Postle, & M. Niwa, Eds., Textile Machinery Society of Japan, Osaka, , 239-250.
- Chamberlain, J. (1949). "Hosiery Yarns and Fabrics", Vol. 2., Leicester College of Technology and Commerce, Leicester, , pp. 107.
- Curiskis, J.I., G. A. Carnaby (1985). Continuum Mechanics of the Fiber Bundle, Textile Research Journal, Vol.55, 334-344
- Carnaby, G.A. (1976). The Structure & Mechanics of Wool Carpet Yarns, Doctoral thesis, University of Leeds,
- De Jong, S. & Posite, R. (1977). Energy Analysis of Woven-Fabric Mechanics By Means of Optimal-Control Theory, Part I: Tensile Properties, Journal of Textile Institute, , Vol. 68, p350-362.
- Demiröz, A., & Dias, T. (2000). A Study of the Graphical Representation of Plain-Knitted Structures, Part I: Stitch Model for the Graphical Representation of Plain-Knitted Structures, The Journal of The Textile Institute, Vol. 91 (4), No. 1, pp. 463-480.
- Demiröz, A., & Dias, T. (2000). A Study of the Graphical Representation of Plain-Knitted Structures, Part II: Experimental Studies and Computer Generation of Plain-Knitted Structures, The Journal of The Textile Institute, Vol. 91 (4), No. 1, pp. 481-492.
- Grosberg, P. and Kedia, S. (1966). The Mechanical Properties of Woven Fabrics, Part I: The Initial Load Extension Modulus of Woven Fabrics, Textile Research Journal, Vol.36 (1), pp71-79.
- Hadizadeh, M., Jeddi, A.A.A. & Tehran, M. A. (2009). The Prediction of Initial Load-extension Behavior of woven Fabrics Using Artificial Neural Network, Textile Research Journal, vol.79, No.17, pp. 1599-1609.
- Hearle, J.W.S., Grosberg, P., & S. Baker (1969). "Structural Mechanics of Fibers, Yarns, & Fabrics, " Vol. 1, John Wiley & Sons, New York, USA.
- Hearle, J.W.S. & Shanahan, W.J. (1978). An Energy Method for Calculations in Fabric Mechanics, Part I: Principles of the Method, Journal of Textile Institute, , 69 (4), pp81-91.
- Hearle, J.W.S. & Shanahan, W.J. (1978). An Energy Method for Calculations in Fabric Mechanics, Part II: Examples of Application of the Method to Woven Fabrics, Journal of Textile Institute, 69 (4), 92-100.
- Huang, N.C. (1978). Technical Report SM7801, Solid Mechanics Group, Department of Aerospace and Mechanical Engineering, University of Notre Dame, U.S.A., Sep.,



- Hursa, A., Rotich, T. & Ražić, S. E. (2009). Determining Pseudo Poisson's Ratio of Woven Fabric with a Digital Image Correlation Method, *Textile Research Journal*, vol.79, No.17, pp. 1588-1598.
- Kurbak, A. (1998). Plain-Knitted Fabric Dimentions, Part II, *Textile Asia*, April, pp. 36-40, pp. 45-46.
- Kurbak, A. & Alpyildiz, T. (2009). Geometrical Models for Cardigan Structures, Part I: Full Cardigan, *Textile Research Journal*, Vol. 79, No. 14, pp. 1281-1300.
- Kurbak, A. & Alpyildiz, T. (2009). Geometrical Models for Cardigan Structures, Part II: Half Cardigan, *Textile Research Journal*, Vol. 79, No. 18, pp. 1635-1648.
- Lekhnitskii, S.G., *Theory of Elasticity of an Anisotropic Elastic Body*, Holden-Day, San Francisco,
- Leaf, G.A.V., & Glaskin, A. (1955). Geometry of Plain-Knitted Loop, *The Journal of The Textile Institute*, Vol. 46, pp. 587-605.
- Leaf, G.A.V. & Kandil, K.H. (1980). The Initial Load-extension Behaviour of Plain-woven Fabrics, *Journal of Textile Institute*, , Vol. 71, No. 1, pp. 1-7.
- Lai, T.-P. (1985). "Practical Fiber Physical Chemistry", Tai-Long Publishing Co. Taipei, ROC,
- Lekhnitskii, S.G. *Theory of Elasticity of an Isotropic Body*, Holden-Day, San Francisco, USA.
- Lin, J. J. (2007), Prediction of Yarn Shrinkage Using Neural Nets, *Textile Research Journal*, Vol.77 (5), pp336-342,
- Munden, D. L. (1961). The geometry of a Knitted Fabric in its Relaxed Condition, *Hosiery Times*, April, Vol. 43.
- Naik, N.K. & Ganesh, V.K. (1992). Prediction of on-axes elastic properties of plain weave fabric composites, *Composite Science and Technology*, Vol. 45, 135-152.
- Peirce, F.T. (1937), *The Geometry of Cloth Structure*, *Journal of Textile Institute*, Vol 28, T45-96.
- Peirce, F.T. (1947). Geometrical Principles Applicable to the Design of Functional Fabrics, *Textile Research Journal*, Vol. 17, pp. 123-147.
- Sun, H., Pan, N. & Postle, R. (2005). On the Poisson's ratios of a Woven fabric, *Composite Structures* Vol.68, pp. 505-510.
- Postle, R. (1971). Structure Shape and Dimensions of Wool Knitted Fabrics, *Applied Polymer Symposium*, No. 18, John Wiley, Chichester, pp. 149.
- Semnani, D., Latifi, M., Hamzeh, S., & Jeddi, A. A. A. (2003). A New Aspect of Geometrical and Physical Principles Applicable to the Estimation of Textile Structures: Ideal Model for Plain knitted Loop, *The Journal of The Textile Institute*, Vol. 99, No. 1, pp. 204-213.
- Thwaites, J.J. (1980). A Continuum Model for Yarn Mechanics, in "Mechanics of Flexible Fiber Assemblies," J.W.S. Hearle, J.J. Thwaites, & J. Amirbayat, Eds., Sijthoff and Noordhoff, Alphen aan den Rijn, The Netherlands,, pp. 87-97.
- Womersley, J.R. & D.I.C., B.Sc. (1937). The Application of Differential Geometry to the Study of the Deformation of Cloth under Stress, *Journal of Textile Institute*, , Vol. 28, T99-113.



## **Woven Fabric Engineering**

Edited by Polona Dobnik Dubrovski

ISBN 978-953-307-194-7

Hard cover, 414 pages

**Publisher** Sciyo

**Published online** 18, August, 2010

**Published in print edition** August, 2010

The main goal in preparing this book was to publish contemporary concepts, new discoveries and innovative ideas in the field of woven fabric engineering, predominantly for the technical applications, as well as in the field of production engineering and to stress some problems connected with the use of woven fabrics in composites. The advantage of the book Woven Fabric Engineering is its open access fully searchable by anyone anywhere, and in this way it provides the forum for dissemination and exchange of the latest scientific information on theoretical as well as applied areas of knowledge in the field of woven fabric engineering. It is strongly recommended for all those who are connected with woven fabrics, for industrial engineers, researchers and graduate students.

### **How to reference**

In order to correctly reference this scholarly work, feel free to copy and paste the following:

Jeng-Jong Lin (2010). Prediction of Elastic Properties of Plain Weave Fabric Using Geometrical Modeling, Woven Fabric Engineering, Polona Dobnik Dubrovski (Ed.), ISBN: 978-953-307-194-7, InTech, Available from: <http://www.intechopen.com/books/woven-fabric-engineering/prediction-of-elastic-properties-of-plain-weave-fabric-using-geometrical-modeling>

**INTECH**  
open science | open minds

### **InTech Europe**

University Campus STeP Ri  
Slavka Krautzeka 83/A  
51000 Rijeka, Croatia  
Phone: +385 (51) 770 447  
Fax: +385 (51) 686 166  
[www.intechopen.com](http://www.intechopen.com)

### **InTech China**

Unit 405, Office Block, Hotel Equatorial Shanghai  
No.65, Yan An Road (West), Shanghai, 200040, China  
中国上海市延安西路65号上海国际贵都大饭店办公楼405单元  
Phone: +86-21-62489820  
Fax: +86-21-62489821

© 2010 The Author(s). Licensee IntechOpen. This chapter is distributed under the terms of the [Creative Commons Attribution-NonCommercial-ShareAlike-3.0 License](https://creativecommons.org/licenses/by-nc-sa/3.0/), which permits use, distribution and reproduction for non-commercial purposes, provided the original is properly cited and derivative works building on this content are distributed under the same license.

IntechOpen

IntechOpen